CEA/SACLAY
DSM

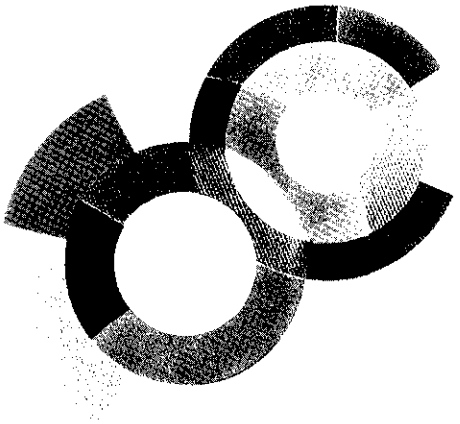

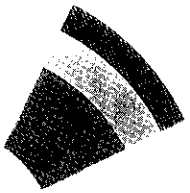

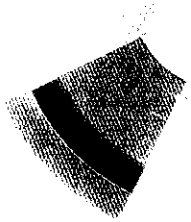

DAPNIA/SPHN-99-11 03/1999

First experiments with the FUSION detector

V. Fekou-Youmbi, J.L. Sida, N. Alamanos, X. Charlot, C. Mazur, A. Mougeot, F. Auger, D. Bazin, C. Borcea, C. Cabot, A. Cunsolo, A. Foti, A. Gillibert, N. Lecesne, A. Lepine, M. Lewitowicz, R. Liguori-Neto, F. Marie, W. Mittig, J.P. Mols, S. Ottini, E.C. Pollacco, A. Ostrowski, M. Riallot, P. Roussel-Chomaz, C. Volant, Y.Y. Feng.

DAPNIA

Submitted to Nuclear Instruments and Methods in Physics Research A

Département d'**A**strophysique, de Physique des **P**articules, de Physique **N**ucléaire et de l'**I**nstrumentation **A**ssociée
CEA/Saclay F-91191 Gif-sur-Yvette Cédex

First experiments with the FUSION detector*

V. Fekou-Youmbi [a], J.L. Sida [a], N. Alamanos [a], X. Charlot [b], C. Mazur [b], A. Mougeot [b], F. Auger [a], D. Bazin [c], C. Borcea [d], C. Cabot [e], A. Cunsolo [f], A. Foti [f], A. Gillibert [a], N. Lecesne [c], A. Lepine [g,c], M. Lewitowicz [c], R. Liguori-Neto [g], F. Marie [a], W. Mittig [c], J.P. Mols [b], S. Ottini [a], E.C. Pollacco [a], A. Ostrowski [c], M. Riallot [b], P. Roussel-Chomaz [c], C. Volant [a] and Y.Y. Feng [h,c]

[a] *Service de Physique Nucléaire, CEA Saclay, 91191 Gif sur Yvette, FRANCE*

[b] *Service Détecteurs, CEA Saclay, 91191 Gif sur Yvette, FRANCE*

[c] *GANIL, B.P 5027, F14021 Caen, France*

[d] *Institute for Physics and Nuclear Enginering, Bucharest Magurke, P.O. Box MG6, Romania*

[e] *IPN Orsay, 91406 Orsay Cedex, France*

[f] *Dipartimento di Fisica and INFN-Sez. CT, 95129 Catania, Italy*

[g] *IFU Sao Paulo, CP 20516, Sao Paulo, Brazil*

[h] *IMP, Academia Sinica, Lanzhou, China*

Abstract

The Fusion Utility for Secondary Ions (FUSION) has been built to measure the fusion-fission cross section induced by radioactive beams at energies around the barrier . A set of ten parallel plate avalanche counters measures the fission fragments which are stopped therein. Twenty plastic scintillators, surrounding the inner shell of PPACs, detect the eventual residue from the projectile. This detector could work in different geometry and allow measurements of low cross section with very weak beams. The measurements at GANIL of the fission cross sections at barrier energies for $^{9,11}Be$ on U are reported.

* Experiment performed at GANIL(CAEN, France)

Preprint submitted to Elsevier Science *2 March 1999*

1 Introduction

Fusion phenomena at low energy are related to the possibility of two colliding nuclei to overcome the repulsive Coulomb barrier which exists between them. This reaction which can only be understood quantum mechanically depends strongly on the structure of the collision partners[1–4]. A global understanding of fusion was proposed in the framework of coupled channel calculations which allow consistent calculations of elastic, inelastic and fusion reactions.

The two remaining major problem were pointed out by M.A. Nagarajan in his concluding remarks of the *Heavy Ion Fusion Conference* held in Padova (May 1994):
Is there a correlation between transfer cross section and fusion enhancement ? Does break-up inhibit fusion or not ?
Radioactive nuclear beams offer a good way to answer these questions by allowing a test of the importance of various effects such as nucleon transfer, break-up or exotic structures like neutron skin or halos.

Several contradictory predictions[6–10] have been proposed for the fusion cross-section of the neutron halo of nuclei, such as ^{11}Li, ^{11,14}Be [5] The presence of this halo can cause a significant enhancement of the sub-barrier fusion cross-sections both because of a lowering of the barrier associated with a stronger nuclear interaction and of an extra enhancement arising from excitation of the predicted soft E1 dipole modes [11]. This enhancement factor might reach 1 or 2 orders of magnitude [6]. The dissociation of the projectile is also predicted to have an influence, with some theories suggesting a strong hindrance to fusion at the barrier [7] while others claim that this will further enhance the fusion probability[9].

2 Choice of the systems

We have planned to measure at GANIL(Caen, France), using the LISE spectrometer [12], the fusion and transfer cross-section for ^{7,9,10,11}Be + ^{238}U at sub-barrier energies. The ^{11}Be presents a one neutron halo, the ^{7}Be is expected to have a large transfer channel influence and the ^{9,10}Be will serve as references. The projectile choice is defined by the secondary beam intensities. At GANIL, secondary beams are produced by fragmentation. The fragmentation cross sections for ^{11}Li and ^{14}Be are too weak to make the primary studies with these nuclei[13]. The two main halo nuclei that can be studied are ^{11}Be and ^{6}He with intensities around 10^5 pps at GANIL energies.

In the fragmentation process, the velocity of the residues is close to the primary

beam velocity. In order to study reactions near the Coulomb barrier, the beam velocity has to be reduced. The best technique to manage this process has been presented previously[14]. In order to limit the reduction of the projectile velocity, and thus the loss of intensity, we have chosen to make the study with a projectile and target which lead to a high Coulomb barrier. This led us to use heavy targets and to make the first studies on the effect of the one neutron halo of the ^{11}Be. Two groups of elements could be used as the target; the first group is lead or bismuth (Z=82,83), the other one is the actinides (Z=90, 92, ...).

A fusion reaction of beryllium with lead or bismuth mainly produces isotopes around radon or francium. The compound nuclei will de-excite via neutron evaporation and then go back to the stability line by alpha emission. A short-lived residual nucleus, after complete or incomplete fusion and neutron emission, could then be identified by its alpha lines. The fusion process has been studied in this way at RIKEN (Japan)[15] and Notre-Dame (USA)[16,17]. The main difficulty in this case is to extract the fusion cross-section, taking into account the different direct reactions and the de-excitation cascade, on the basis of the measurement of some residual nuclei.

The use of actinides presents some advantages:

1. The charge of uranium is higher than lead and thus the loss of intensity due to the reduction in energy of the secondary beams is minimized.

2. The fission cross-section is essentially equal to the fusion cross-section. The fusion-fission probability is of 100% according to the CASCADE code [18] and the GEMINI code [19] for excitation energies above 10 MeV. It varies with the excitation energy of the compound nucleus from 100 % above the barrier to 80 % below the barrier, at 20 MeV excitation energy, according to a code from GSI (Darmstadt) [20]. The important conclusion of these calculations is that fission will occur in more than 80% of the cases and that this probability of fusion-fission does not change more than a few percent, for two isotopes which differ by two nucleons for excitation energies higher than 10 MeV.

3. The fission fragments have some specific characteristics that make them easy to identify. They are heavy nuclei with an energy around 100 MeV. Their range and velocity are very different from those of the projectile or of an evaporated particle. Due to the large mass difference between the projectile and the target, the two fission fragments (noted *ff*) are emitted near 180° in the laboratory. The detection of these fragments will provide the fission cross section.

Transfer or inelastic reactions could also lead to the fission of the system. In order to discriminate between fusion and other reactions, the remaining part of the projectile must be detected with a very high efficiency. The presence

of a projectile residue (noted *rp*) will be the signature of a transfer reaction, while its absence will show complete fusion.

3 Signature of the events

The range and the velocity of the particles are the parameters which allow the best separation between fission fragments and residual projectiles. The fission fragments have a number of protons between 35 and 60 and a kinetic energy distribution between 60 and 150 MeV. A residue from the projectile will have a charge close to the charge of the projectile, in our case 4, and an energy below 50 MeV for the sub-barrier studies. The ranges of these two species are different by one order of magnitude: 10 mg/cm^2 for a 50 MeV $^{10}_{4}$Be and 0.2 mg/cm for a 150 MeV $^{90}_{35}$Br, which corresponds to extreme conditions of fission. The measurement of ranges is very difficult and this parameter will be grossly used in the building of the detector. A first shell of detection will measure and stop the fission fragments, while a residue from the projectile will pass through. The second shell of detection will stop the possible projectile residue.

The velocity of these two types of particles, *ff* and *rp*, will serve as a better parameter for disentangling them as shown in [21]. Fission fragments have velocities of the order of 1cm/ns, whereas residues from the projectile have velocities close to the beam velocity, *i.e.* around 3 cm/ns for 50 MeV ^{10}Be. It will be difficult to separate *ff* and *rp* with only the velocity parameter for beam energies four times lower, around 10 MeV.

The time of flight and position will be measured. The measurement of the position of the fission fragments will also provide the angle between the two fission fragments which is a very selective parameter for the signature of a fission event.

A discrimination via the total energy measurements has not been used due to the large energy distribution of the fission fragments. For high energy projectiles, they could be mixed with *rp*. A measurement of energy loss and energy could be very valuable but it would multiply the number and the cost of the detectors.

Fusion could also be studied by measuring the velocity of the recoil nucleus. As discussed before, we want to make the study with a heavy target and light projectiles. In that case, the discrimination between a transfer reaction and fusion is very difficult. The velocities of the different compound nuclei are very close and, due to strong variations of the angular distribution for energies around the barrier, it is difficult to identify the contribution of fusion

and transfer. As an example, for energies above the barrier the velocity of the fusion recoil nuclei are faster than the transfer ones and, at energies below the barrier, it is the opposite [21]. Furthermore, this technique needs a minimum of straggling, so the use of thin targets, which are not compatible with the weak intensity of radioactive beams.

In summary, we decided to study the fusion probability for the isotopes of beryllium on a target of ^{238}U and to define a fusion event as a fission without residue from the projectile. For this purpose, the time of flight is measured for both *ff* and *rp*. In order to calculate the angle between the *ff*, their positions are measured as well.

4 The F.U.S.ION detector

4.1 General information

The FUSION detector (Fusion Utility for Secondary Ions) has been developed at Saclay (France) for this purpose. This detector could be placed in two different configurations according to the expected counting rates. The first one has the structure of a box of detection, with one or three targets inside. The second one, the in-line configuration, is an alternating sequence of targets and detectors. It could run with five targets at the same time. Each configuration is an arrangement of a first stage of detection with parallel plate avalanche counters (PPAC) for the fission fragments followed by fast plastic scintillators for the possible light particle, residue from the projectile. An absorber is placed between these two types of detectors to be sure that the fission fragments do not reach the plastics. The threshold on the PPACs made them insensitive to light particles.

Since fusion is defined by the absence of projectile-residue, each configuration must cover a solid angle as large as possible for this measurement in order to minimize uncertainties. On the other hand, due to the low intensity of the secondary beams and the weak cross section we have to measure fission fragments also with the largest solid angle possible. For the two configurations presented below, the optimization of the solid angle was of major importance.

In general, secondary beams produced by fragmentation have a large emittance. The size spot on the target was estimated to be of 2 cm. Furthermore, we want to measure time of flight. These two conditions lead us to a typical size of the detectors of 30 cm to be not to sensitive to the beam spot and to have a sufficient flight path without too many mechanical constraints correlated with a very large detector.

The weak intensity of the radioactive beams requires the use of thick targets. For fission studies, the thickness is limited by the range of the fission fragment. The thickness seen by the fission fragments depends of the angle of emission. The target introduces a dead zone in the region where the fission fragments will not get out or have not enough energy to reach the active part of the detector. A measurement has been made of this dead zone for a 1mg/cm^2 thorium target made by rolling and compared with a simulation. In figure 1, the efficiency is presented as a function of the target thickness according to a simulation, points fitted by a straight line, which is in agreement with our measurement (square). The simulation is a fission fragment generator inside the target medium. The charge, mass and energy are generated randomly according to fission fragment distributions [22]. The ranges of the fragments are determined by the TRIM code [23]. The calculation is an overestimation of the efficiency since fission fragments are bare nucleus at their production so have a lower range than ions with a charge state at equilibrium which are taking into account in the TRIM calculation. Our conclusions were that a 1 mg/cm^2 target could be used with a dead zone of 10° on each side of the target plane.

Due to the large emittance, a target of more than 2 cm is necessary. For such a large surface, the desired thickness is difficult to reach: too thick for evaporation and too thin for rolling . The targets for the real experiment were of 2 μm (1.6 mg/cm^2) U3O8, which is equivalent to 1 mg/cm^2 of U. They were made by electron sputtering on a thin plastic film where a few angstroms of gold were evaporated in order to improve the adhesion[24].

4.2 The two configurations

4.2.1 The box

In the box configuration, figure 2, the detector is composed of two open cubes on each side of the target plane. The distance target-PPAC, between 15 and 35 cm, allows a good measurement of the time of flight for the fission fragments. The maximum size of the set-up was defined by the aperture of our reaction chamber : 700x700 cm^2. The geometrical efficiency of the set-up is 75 %. In the 10° dead zone of the target-plane all the mechanics for the target, the mechanics and electronics for the PPACs have been placed.

The box set-up could run with one or three targets. In the one target configuration, the target is at the center of the detector. In the three targets configuration, two other targets which are remote controled, came in the beam at +/- 15 cm of the center of the detector. This configuration allows measurement at three energies at the same time. The three steps in energy are defined by

the energy loss in each target, 1 MeV for the targets described previously. The coincidence between the two fission fragments is necessary to define the target which has been fired via the mean position on the beam axis. The resolution of 5 mm allows us to recognize without ambiguity which target fired. The total number of fission is improved by a factor of two in the three targets configuration as compared to one target.

4.2.2 The in-line configuration

Another configuration for very low counting rates has been prepared and studied, the in-line configuration, figure 3. Five targets could be used. Each target is the center of a sandwich of plastics and PPACs. The PPAC detectors at 5 cm from the target define the same solid angle as in the box. All the detectors are normal to the beam and are crossed by the beam. When the beam passes through a target, approximately 1 MeV is lost and 1.7 MeV are lost by passing through a PPAC. In a single measurement, five energies are measured at the same time. The target where the fusion occured is identified by the PPACs fired by fission fragments. The time of flight measurement is not relevant due to the small flight path. The angle between the fission fragments will define a fission event. Due to all the material crossed by the beam, the beam suffers a large straggling, which is a difficulty in measurements where the cross-sections vary rapidly with energy.

4.3 Detector characteristics

4.3.1 Parallel plate avalanche counters

The parallel plates developed for the FUSION detector have an active area of 290x290 mm^2 for a size of 370x370 mm^2. They are made of three electrodes which are 1.5 μm Mylar foils metallized with gold. Two of them, the anodes, are stripped in 57 bands of 5 mm. The third one, metalized on all the surface and on both sides, is the cathode and is placed between the two anodes. The strips of the two anodes are orthogonal. The anode-cathode distance is 3 mm. The typical high voltage is 500 V on the cathode, while the anodes are at ground. The strips are connected to a delay line with a 5 ns step. The two extremities of the delay lines are read. By time difference with the cathode signal, the position of the strip fired is determined for the two orthogonal anodes. The precision on the position of the passage of a particle is a pixel of 5x5 mm^2 on the plane of the PPAC. This set of electrodes is in a low isobutane pressure environment (4.5 Torr). The thickness of the window foil of the PPAC is 2.5 μm Mylar. This low thickness was necessary to maximize the efficiency for fission fragment measurement. Four wires have been used to

limit the deformation of the window foils. Tests have been made for pressure up to 10 Torr without breaking these foils. The foils have not been glued as usually. They were maintained by double-face tape which is easier to remove in case of any relevant problems.

The two configurations of detection requires that the beam is passing through some of the PPACs. The cathode of these PPACs has not been metalized on a disk of 5 cm. The electric field is close to zero in this area. The number of crossed PPACs is different in the two configurations, two for the box and ten for the in-line one. To change from one configuration to another, we have to change some of the cathodes. In order to do it rapidly, the three electrodes are a sandwich independent of the housing of the detector and, instead of changing only the cathode, we change the set of electrodes. We have only to take out the entrance window, take the group of electrodes, put in the other ones, and close the detector.

The large surface of the detector induces a high capacitance, which requires specific electronics. Fast amplifiers have been developed with a gain of 200. The constant fraction discriminators used, FCC8 from Ganelec, have been modified to improve the time resolution. A fraction of .5 has been used instead of the usual .2 value. The delay have been chosen as 80 % of the rise time, so 2 ns for the cathode and 3 ns for the anode.

The PPAC detector provides a time and a charge via the cathode signal and a position via the two anode signals.

4.3.2 Fast plastic scintillators

Each PPAC is covered by two plastic scintillators, NE102 of area 340x170 mm^2 large and a thickness of 8 mm. Two plastic detectors were chosen instead of one in order to optimize the time resolution, which is 1 ns. In order to minimize the dimension of the FUSION set-up, the light guide made a rotation of 90 ° to reach the photomultiplier (figure 2). Photomultipliers are then very close to the PPAC. Electric (copper) and magnetic (mu-metal) screens have been developed to avoid cross-talk between the two types of detectors. The cross-talk and noises on the PPACs due to the PM fast signals have been suppressed. After calibrations, the evolution with time of the PM gain and the proper functioning of the plastics have been monitored with a light generator and optic fibers connected to the light-guides. As for PPACs, some of the plastics are crossed by the beam. Due to the high thickness of the plastics, there is no solution except to make a hole in the plastic. A conic hole has been made for all the plastics that can be opened or closed with an adapted conic piece of scintillator. When a Cs source is collimated on this piece, the loss of light as compared to a plastic without the hole is only 10 %.

5 Tests of the detectors

5.1 Fission measurement

A first test was made with a californium source on a thin support. The californium could fission spontaneously and, due to the thin support, the two fission fragments could be detected in coincidence in the PPACs. The charge, position, and time of flight difference between the set of front PPACs and the back ones were measured. Plastic scintillators were never fired by fission fragments. This is a validation of our gross range selection. The charge deposited in the PPACs, the time of flight and the position are measured. On figure 4, the two-dimensional plot presents the time difference as a function of the angle between the two fragments. The angle distribution is clearly peaked around 180°. The two peaks, corresponding to the fission-fragment mass distribution, are clearly seen. The time resolution is much better than the charge resolution[25]. Due to the large distribution of fission fragments it is difficult to extract precise values of the resolution with such a method. Tests with alpha and in coincidence with another start detector give us an intrinsic typical resolution of 1 ns. The charge resolution is not relevant as this resolution is different for alpha and fission fragments.

5.2 Projectile residue measurement

The set of plastic scintillators has been tested with elastic scattering of a composite beam of ^{9,10}Be, ^{8}Li and ^{10}B with the same magnetic rigidity of 0.8470 Tm (figure 5). The high frequency of the cyclotron was used as a reference. The different particles from the beam are clearly separated in the time of flight measurement.

The charge detected in plastics is calibrated with cosmic muons and with the scattered beam. This calibration depends of the nature of particle. The charge resolution was of the order of 20%.

6 First measurements

The first experiment done with the FUSION set-up was the study of ^{9,11}Be+^{238}U systems. The configuration used for the first experiment was the box with only one target in order to start in optimized conditions.

In order to determine a cross section for a specific reaction it is necessary to

take care of impurities in the secondary beam. For each run, the beam purity was higher than 95% and in general closer to 98%, due to selection of the secondary beam in the LISE spectrometer with a degrader in the intermediate focal plane and by velocity selection in the Wien filter LISE3 [26]. The momentum aperture was $\Delta P/P = \pm 2.5\%$. A ^{11}Be beam intensity of 2 10^3 has been obtained at 5 MeV/A (figure 6).

The beam impinges on a 1.6 mg/cm^2 U_3O_8 target. The heavy reaction products fire the PPACs. The relative angle beetween coincidence events in two PPACs as a function of the relative time of flight is presented in figure 7 for the different measurements. Fission fragments are peaked around 180°. In addition, the relative time of flight provides a good complementary selection. The selection of the fission events corresponds to a box which is drawn for each measurement. Background events have been measured during a six hours run during which no contamination events were seen in the fission selection. This provides a good confidence level even for measurements with very low statistics (2 fission events in ^9Be at $E_{cm} = 38.82\ MeV$ and in ^{11}Be at 37.35 MeV).

The start detector for the time of flight measurement, an in-beam CsI foil with micro-channel plates, was not working properly. We attempted to replace it with the high frequency from the cyclotron, but for secondary beams at low velocity and full momentum aperture this time reference is inappropriate. For a secondary beam produced at the entrance of the LISE spectrometer, the flight path is of the order of 60 m which corresponds to a time of 2 μs. For an aperture of the spectrometer of $\Delta P/P = 5\%$, the time fluctuation of the secondary beam is 100 ns, thus comparable to the HF period. The information from plastics where not useable. Thus, only fission cross sections for $^{9,11}Be + ^{238}U$, measured in the PPACs, have been extracted (figure 8) for statistics higher than one event. The error bars plotted are only due to statistics. The energies are corrected for the energy lost in the target.

For the ^9Be projectile, there is no doubt that the main part of the fission cross section comes from fusion. Thus, the normalizaton of the measurements on that system via calculated fusion cross sections for energies slightly above the barrier is justified. In the present case, the normalization has been obtained with the calculation of the fusion cross section for ^9Be at 48.59 MeV. The potential has been calculated by the double-folding method with the M3Y nucleon-nucleon interaction [27]. The densities of ^9Be and ^{238}U were extracted from electron scattering measurement [28]. The first 2^+ state at 44.9 keV ($B(E_2) = 12.3\ e^2b^2$) [29] and 4^+ at 148.4 keV ($B(E_4) = 0.69\ e^2b^4$) [30] of ^{238}U were coupled in the fusion calculation. The theoretical values are in agreement with the fission cross section measured for $^9Be + ^{235}U$ at $E_{LAB} = 50$ and $53 MeV$ by A. Kailas *et al* [31]. This calculation provide a general normalization since the experiment has been done in the same conditions for the two isotopes and the different energies. The fission conditions, angle and velocity

of the fission fragments, support very small variations with the energy of each isotopes.

We observe for the two systems that the cross section is lower than predicted by the calculation at energy above the barrier. This could be due to the break-up influence as seen for $^{9}Be + ^{208}Pb$[32]. At energies below the barrier, the fission cross section for the halo nucleus seems to be higher. This unusual trend of the fission cross section could be due : to the feeding of fission via transfer reactions or to an effect on the fusion process. In the first hypothesis, the first shoulder must be due to the fusion feeding where the second one must be due to transfer reactions such as pointed out previously [33]. In the second hypothesis, the increase could be correlated to the low binding energy of the last neutron.

In both hypotheses, we must conclude that the fusion cross section is not abnormaly enhanced by the diffuse density of the projectile nucleus at barrier energies and above the barrier. At lower energies, $E_{cm} = 40$ MeV, the fission probability for ^{11}Be seems to be ten times higher than for ^{9}Be. The point at 38 MeV corresponds to only two fission events so suffer for a lack of statistics even if these events are in a clean space of the two-dimensional plot.

Some measurements have been done also on the $^{6}He + Bi$ system. In the Bi(^{6}He,4n) channel *"no effects due to the neutron skin of ^{6}He are observed"* [16]. Surprisingly, in the Bi(^{6}He,3n) channel *"a large enhancement of sub-barrier fusion was found, implying a striking 25% reduction in the nominal fusion barrier."* [17]. Furthermore, some hindrance of the fusion cross section has been observed in studying the $^{9}Be + ^{208}Pb$ system and was correlated to a high break-up probability[32]. This contradictory results show that no clear answer has been found yet on the effect of the diffuse density and of the break-up on the fusion probability.

7 Conclusion

A detector adequate to measure fusion cross section at very low counting rate has been developped with very satisfying tests. It could be used in two different configurations as function of the expected counting rate. One, three or five targets could be used at the same time. Relative fission cross sections were obtained for $^{9}Be + ^{238}U$ and $^{11}Be + ^{238}U$ using the box configuration of the detector. No clear answers could be provide on the effect of weakly bound nucleons on the fusion process close to the barrier.

We would like to thank R. Verna and J.D. Hinnefeld for their carefull reading of the script.

References

[1] R.G. Stokstad et al., Phys. Rev. Lett. 41 (1978) 465
R.G. Stokstad et al., Phys. Rev. C21 (1980) 2427.

[2] M. Beckerman, Phys. Rep. 129 (1985) 145.

[3] S.G. Steadman and M.J. Rhoades-Brown, Ann. Rev. Nuc. Part. Sci. 36 (1986) 649.

[4] M. Beckerman, Rep. Prog. Phys. 51 (1988) 1047.

[5] I. Tanihata et al., Phys. Rev. Lett. 55 (1985) 2676
I. Tanihata et al., Phys. Lett. B160 (1985) 380.

[6] N. Takigawa and H. Sagawa, Phys. Lett. B265 (1991) 23
N. Takigawa, H. Sagawa and T. Shinozuka, Nuc. Phys. A538 (1992) 221c.

[7] M. S. Hussein, M.P. Pato, L.F. Canto and R. Donangelo, Phys. Rev. C46 (1992) 377.

[8] N. Takigawa, M. Kuratani and H. Sagawa, Phys. Rev. C47 (1993) 2470.

[9] C.H. Dasso and A. Vitturi, Phys. Rev. C50 (1994) R12.

[10] W. von Oertzen and I. Krouglov, Phys. Rev. C53 (1996) R1061

[11] S.A. Fayans, Phys. Lett. B267 (1991) 443.

[12] R. Anne et al., Nuc. Instr. Meth., A257 (1987) 215

[13] K. Summerer, Phys. Rev. C, (1990)

[14] Yang Yong Feng et al., Nuc. Instr. Meth. , B82 (1993) 175.

[15] A. Yoshida et al., 1996 Phys. lett. B389 457
C. Signorini et al., Eur. Phys. J. A2 (1998) 227

[16] P.A. DeYoung et al., Phys. Rev. C58 (1998) 3442

[17] J.J. Kolata et al., Phys. Rev. C57 (1997) R6

[18] F. Pülhofer, Nuc. Phys. A280 (1977) 276

[19] R.J. Charity et al., Nucl. Phys. A483(1988) 371

[20] J. Benluire, A. Grewe, M. de Jong, K.-H. Schmidt and S. Zhdanov, Private communication

[21] J.P. Lestone et al., Nuc. Phys., A509 (1990) 178

[22] R. Vandenbosch and J.R. Huizenga, Nuclear Fission, Academic Press 1973

[23] J.F. Ziegler et al., TRIM code, Stopping powers and ranges in all elements, Pergamon Press 1977,1980,1985

[24] IRMME, Geel, Belgique

[25] V. Fekou-Youmbi et al., Nuc. Phys. A583 (1995) 811c.
V. Fekou-Youmbi et al., J. Phys. G 23 (1997) 1259

[26] A.C. Mueller and R. Anne, NIM B56/57 (1991) 559.

[27] G.R. Satchler and W.G. Love, Phys. Rep. 55 (1979) 183.

[28] C.A. Jager et al., ADNDT 14 (1974)

[29] F.K. McGowan et al., Phys. Rev. Lett. 27 (1971) 1741

[30] D.L. Hendries et al., Phys. Rev. Lett. 31 (1973) 478

[31] S. Kailas et al., Phys. Rev. C42 (1990) 2239

[32] M. Dasgupta et al., Phys. Rev. Lett. 82 (1992) 1395

[33] S.C. Pieper, M.J. Rhoades-Brown and S. Landowne, Phys. Lett. B162 (1985) 43.

Figure Captions

Figure 1 : Evolution of the Efficiency of ff detection with thickness of the metallic Thorium target. The points fitted by the straight line are the results of a simulation. The square corresponds to a measurement.

Figure 2a : Schematic cut view of the FUSION detector in the box configuration. The target is at the center of the detector. There is two shells of detection. The inner shell of PPACs measures the fission fragments. They are surrounded by a shell of plastics which measure the eventual residue from the projectile. The beam is coming from the left and is stopped in a plastic detector which provide the normalization.

Figure 2b : Drawing of the FUSION detector in the box configuration. The shell of plastics is clearly seen with their PM tubes at 90. At the entrance and exit there is a hole in the plastics for the beam. The detectors are on rails(red lines) in order to place everything easily and to change from one configuration to another with the same mechanics.

Figure 3 : Drawing of the FUSION detector in the in-line configuration. The twisted light-guide and PM are clearly seen for each plastic. The targets are not represented. The PPACs are the boxes centered in the beam line. Two PPACS surround a target. Five targets could be used in this configuration.

Figure 4 : Angle beetween the two fission fragments versus their time of flight difference measured with the FUSION set-up for a californium source.

Figure 5 : Time of flight of a scattered composite beam measured in different plastics of the FUSION set-up. The time reference was the high frequency of the GANIL CSS2 cyclotron.

Figure 6 : Evolution of the counting rates of the secondary beams in the first experiment. The full aperture of the LISE spectrometer has been used, $\Delta p/p = 2.5\%$.

Figure 7 : Angle beetween the two fission fragments versus their time of flight difference measured with the FUSION set-up for ^{9}Be and ^{11}Be at different beam energies. The box corresponds to the fission selection. The result of a six hours background measurement is also reported (lower right).

Figure 8 : Energy distribution of the fission cross section. The line corresponds to a coupled channel calculation for $^{9}Be + ^{238}U$.

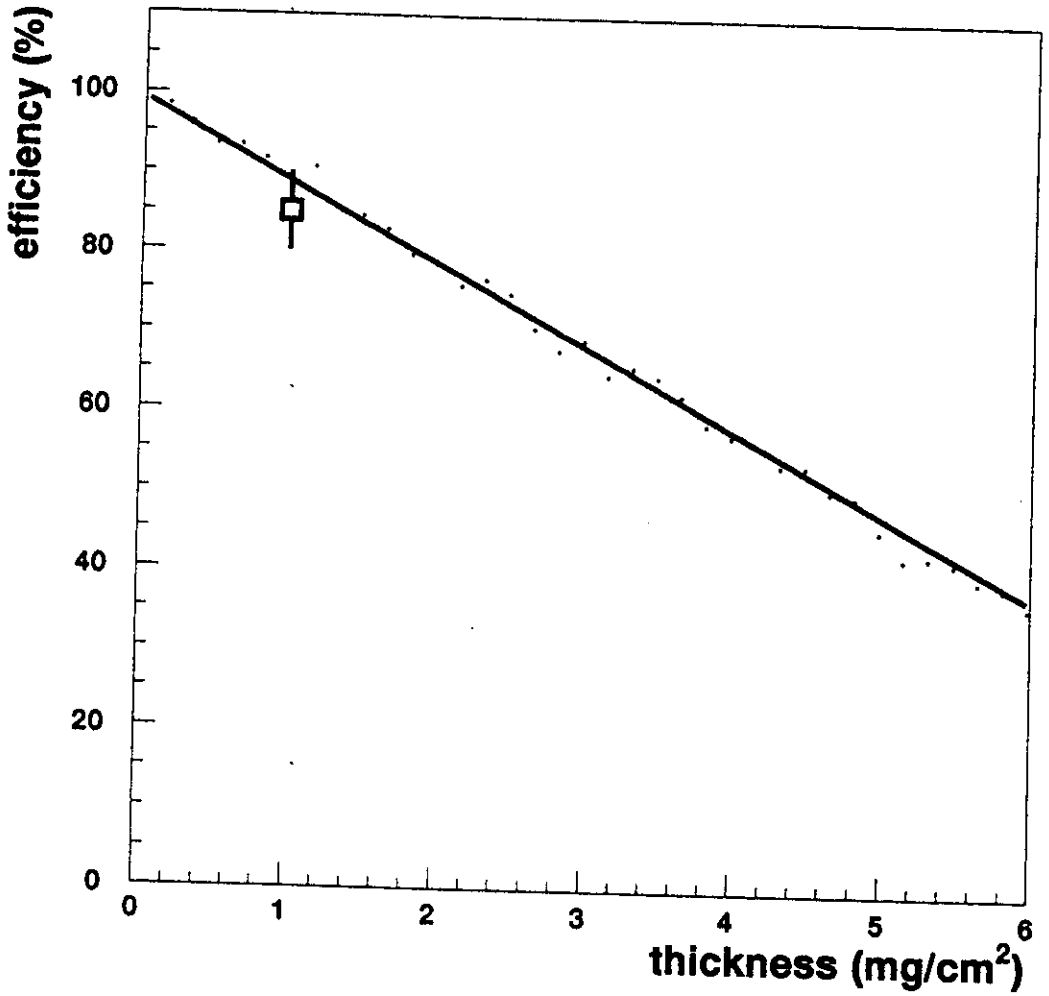

Figure 1

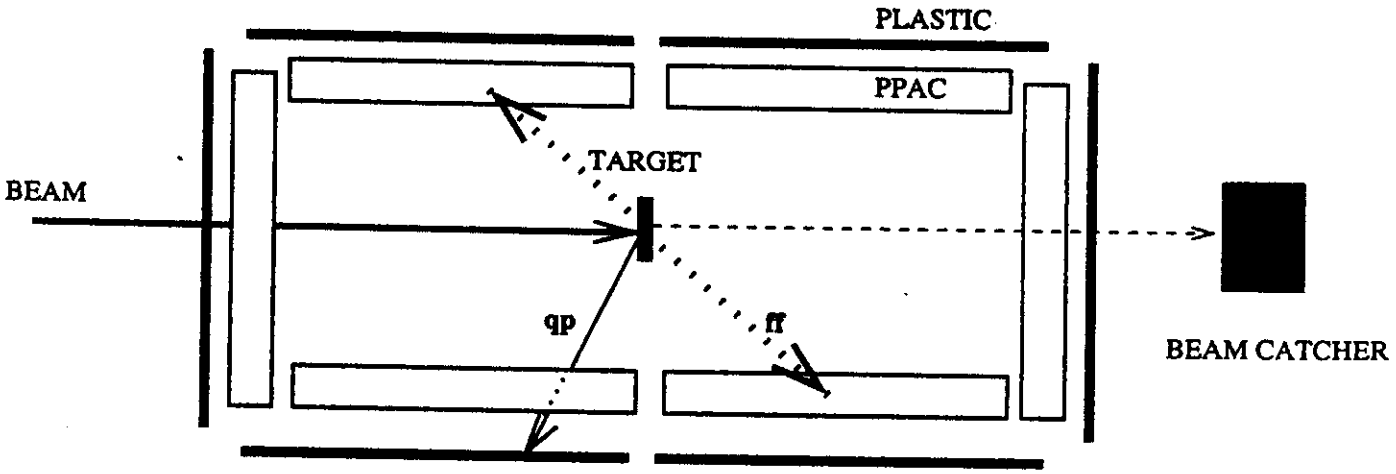

Figure 2a

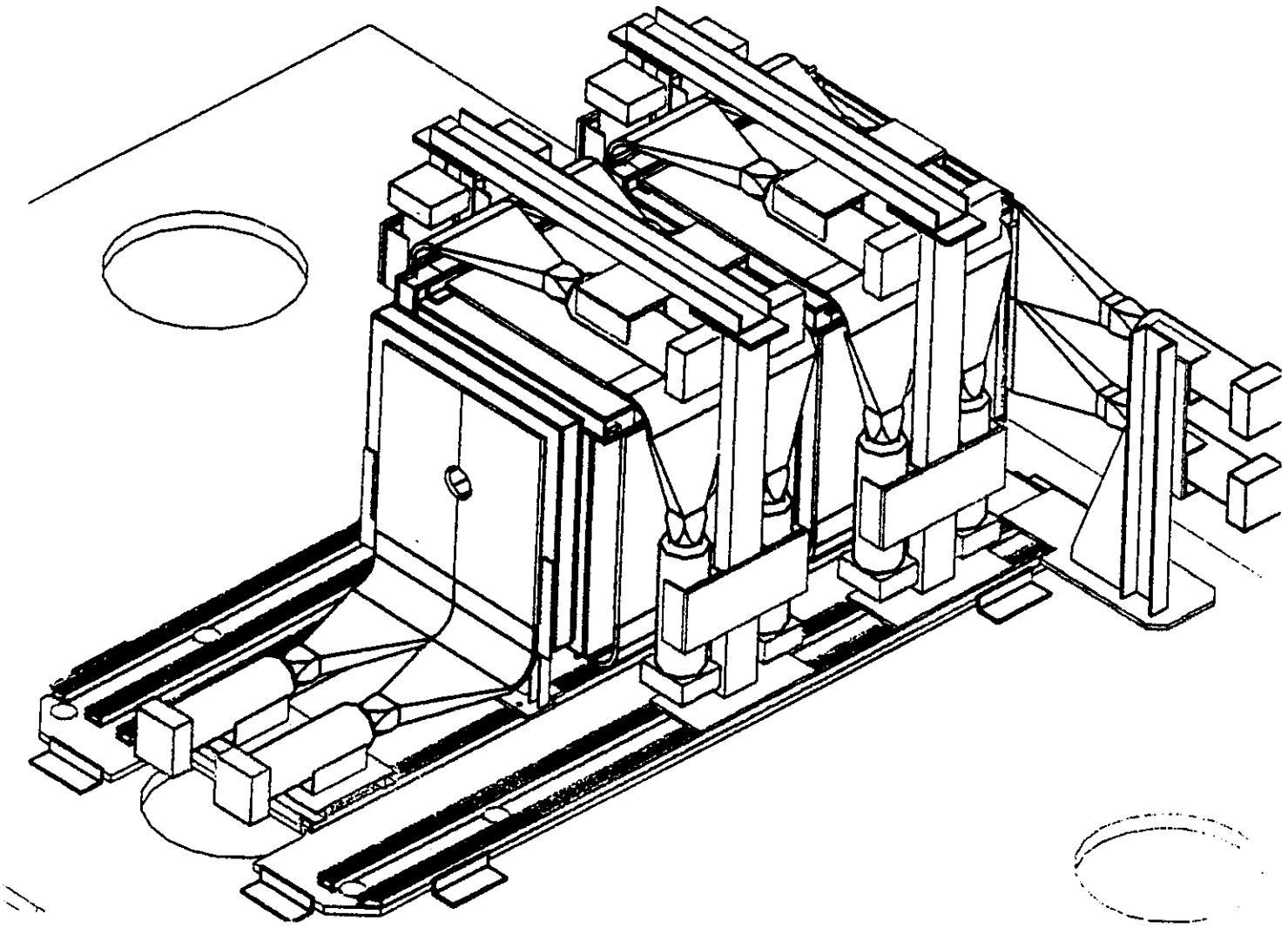

Figure 2b

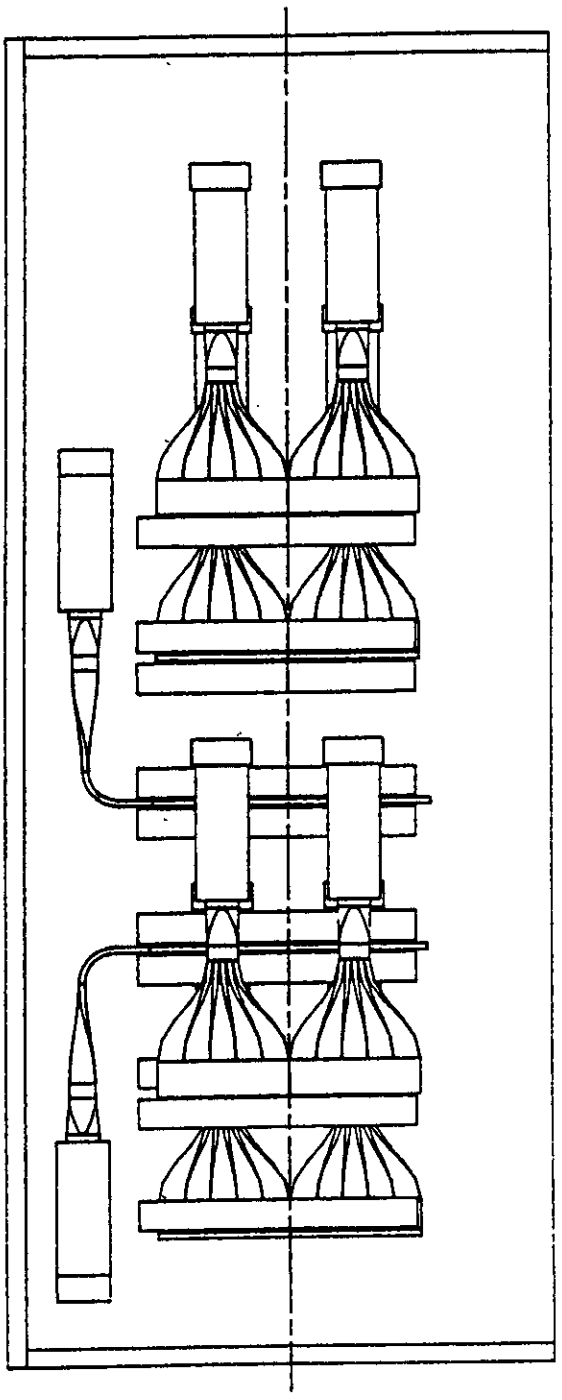

Figure 3

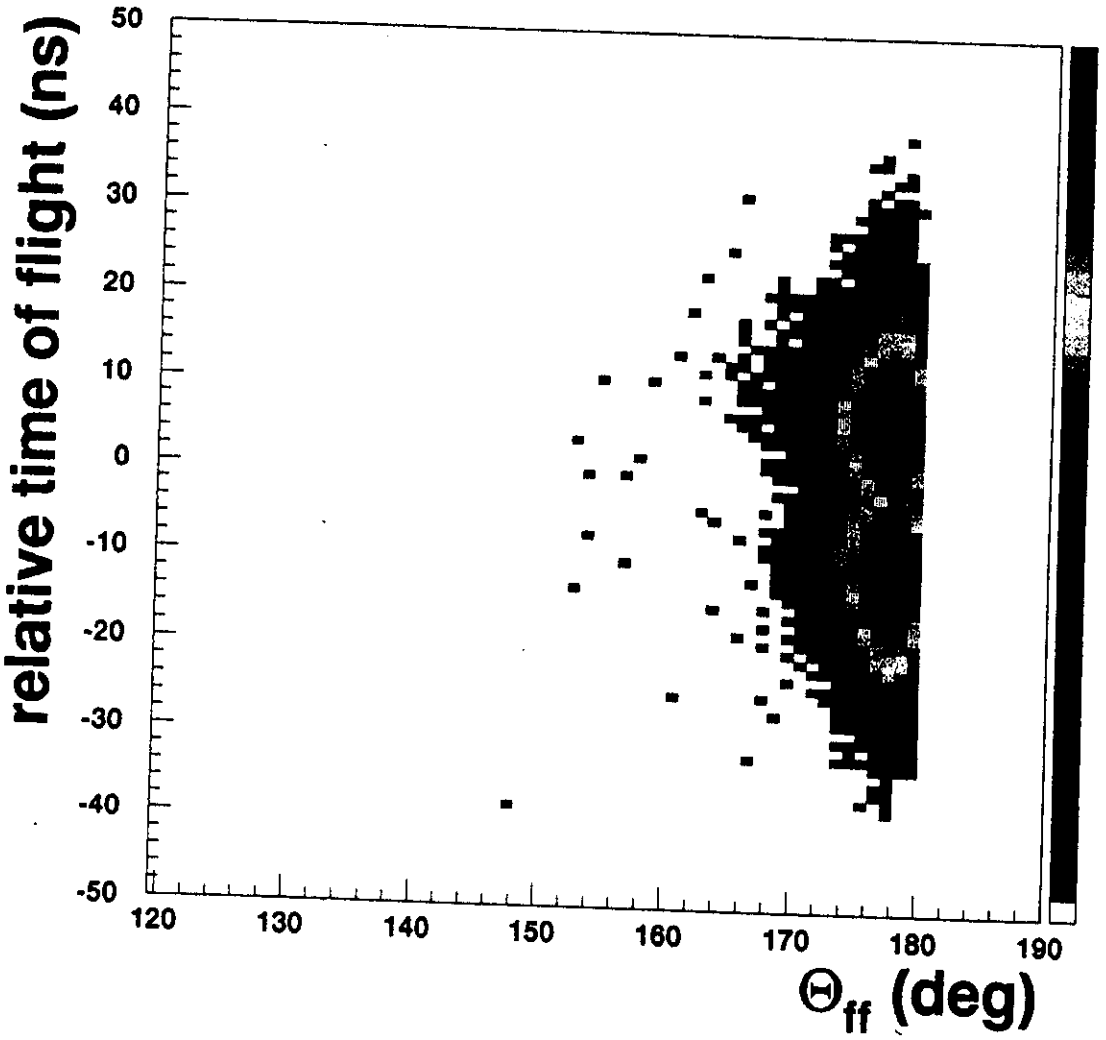
relative time of flight (ns)
50
40
30
20
10
0
-10
-20
-30
-40
-50
120
130
140
150
160
170
180
190
Θff (deg)

Figure 4

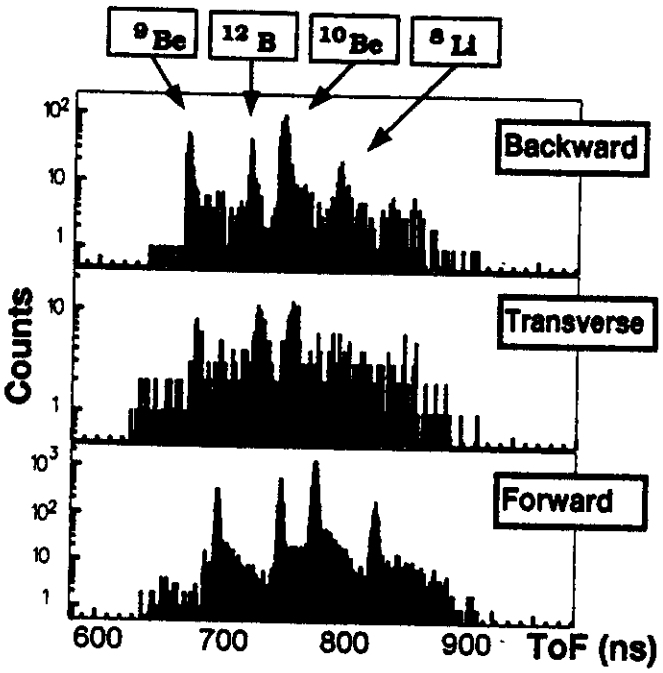
^{9}Be
^{12}B
^{10}Be
^{8}Li
Backward
Transverse
Forward
Counts
10^2
10
1
10^3
600
700
800
900
ToF (ns)

Figure 5

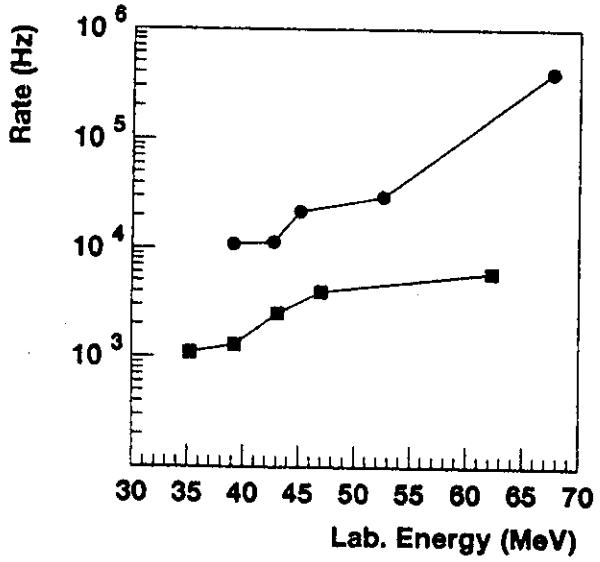

Figure 6

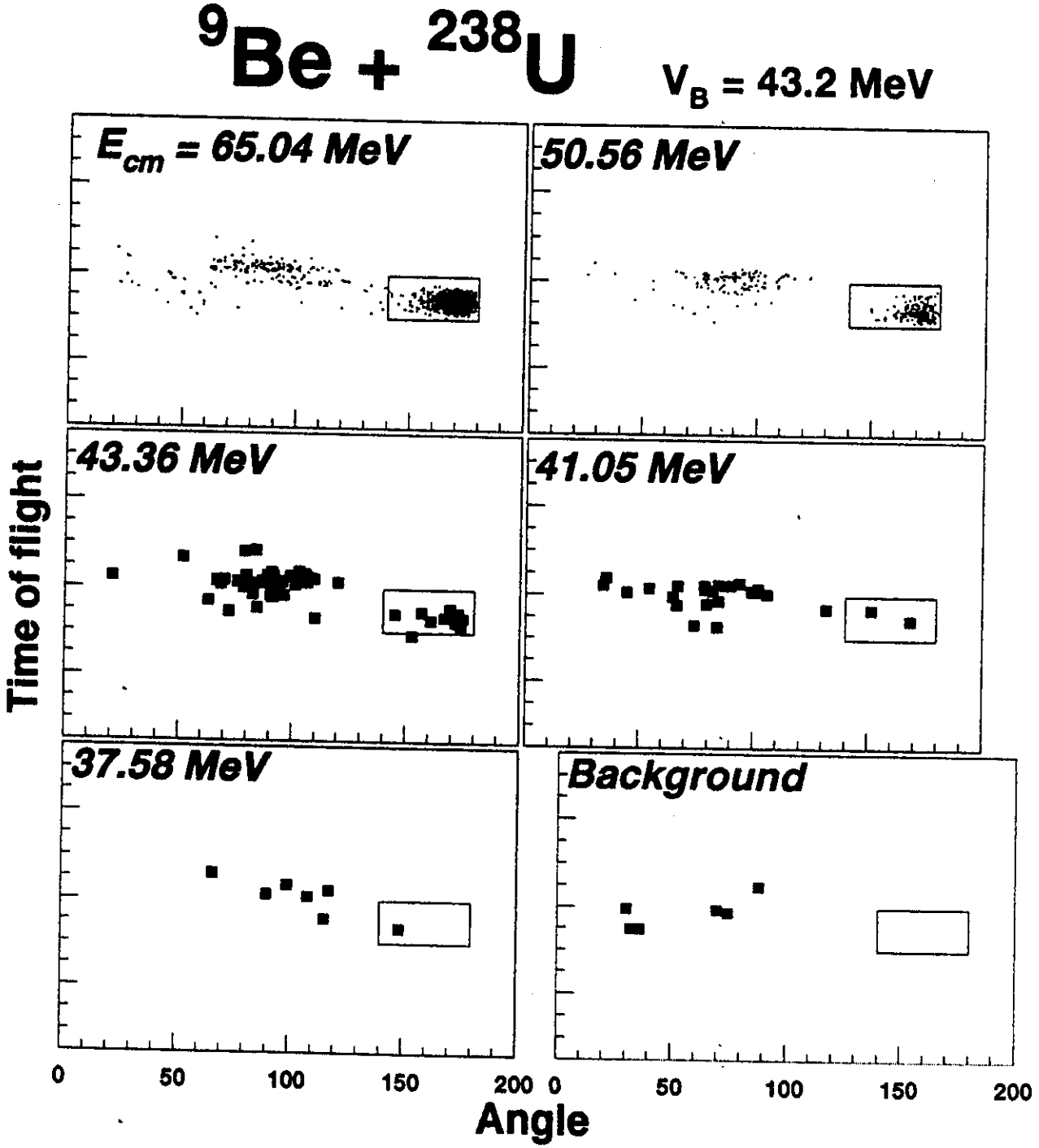
$^{9}Be + ^{238}U$
V_B = 43.2 MeV
E_{cm} = 65.04 MeV
50.56 MeV
43.36 MeV
41.05 MeV
37.58 MeV
Background
Time of flight
0
50
100
150
200
Angle

Figure 7a

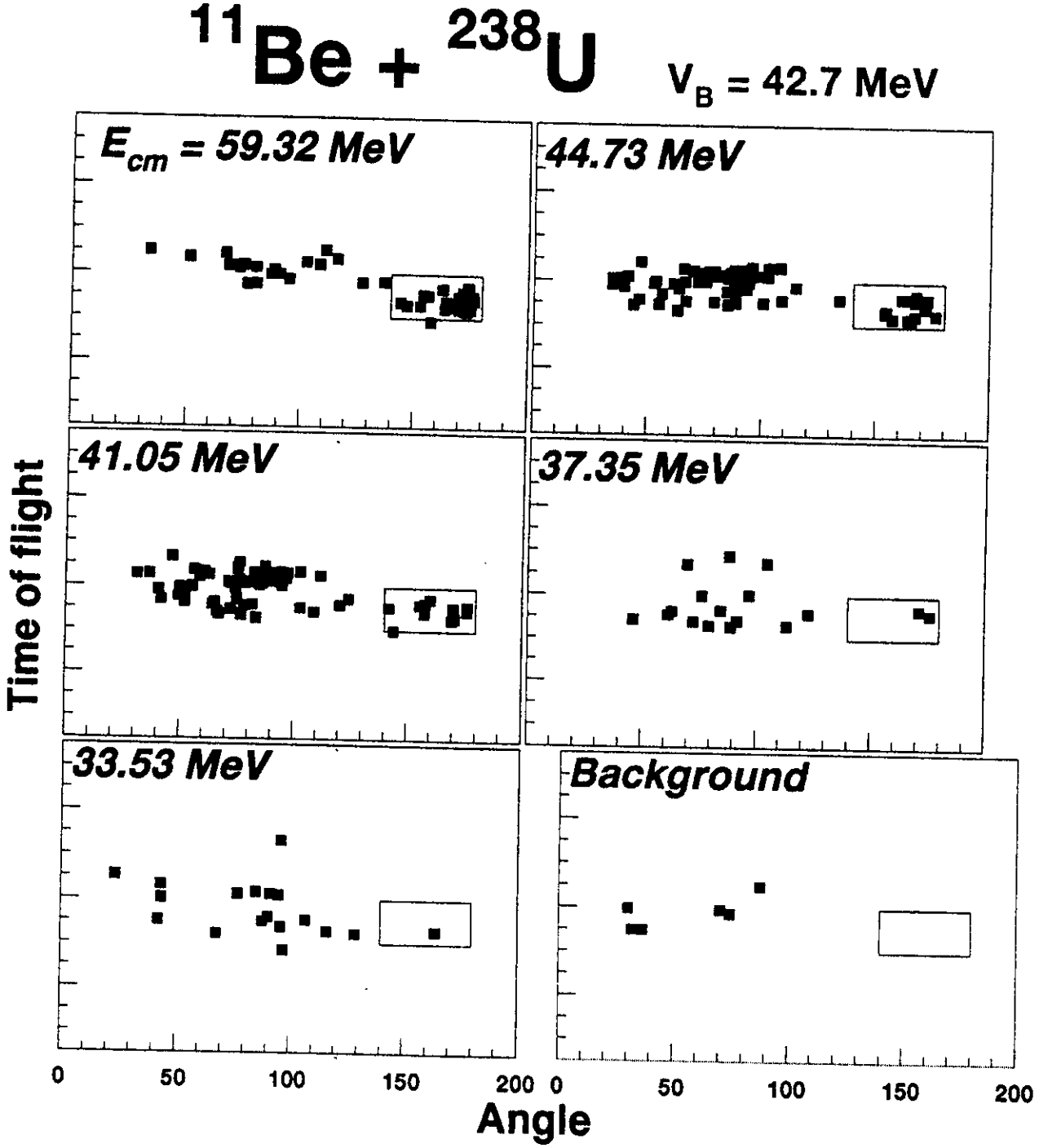
$^{11}Be + ^{238}U$
V_B = 42.7 MeV
E_{cm} = 59.32 MeV
44.73 MeV
41.05 MeV
37.35 MeV
33.53 MeV
Background
Time of flight
0
50
100
150
200
Angle

Figure 7b

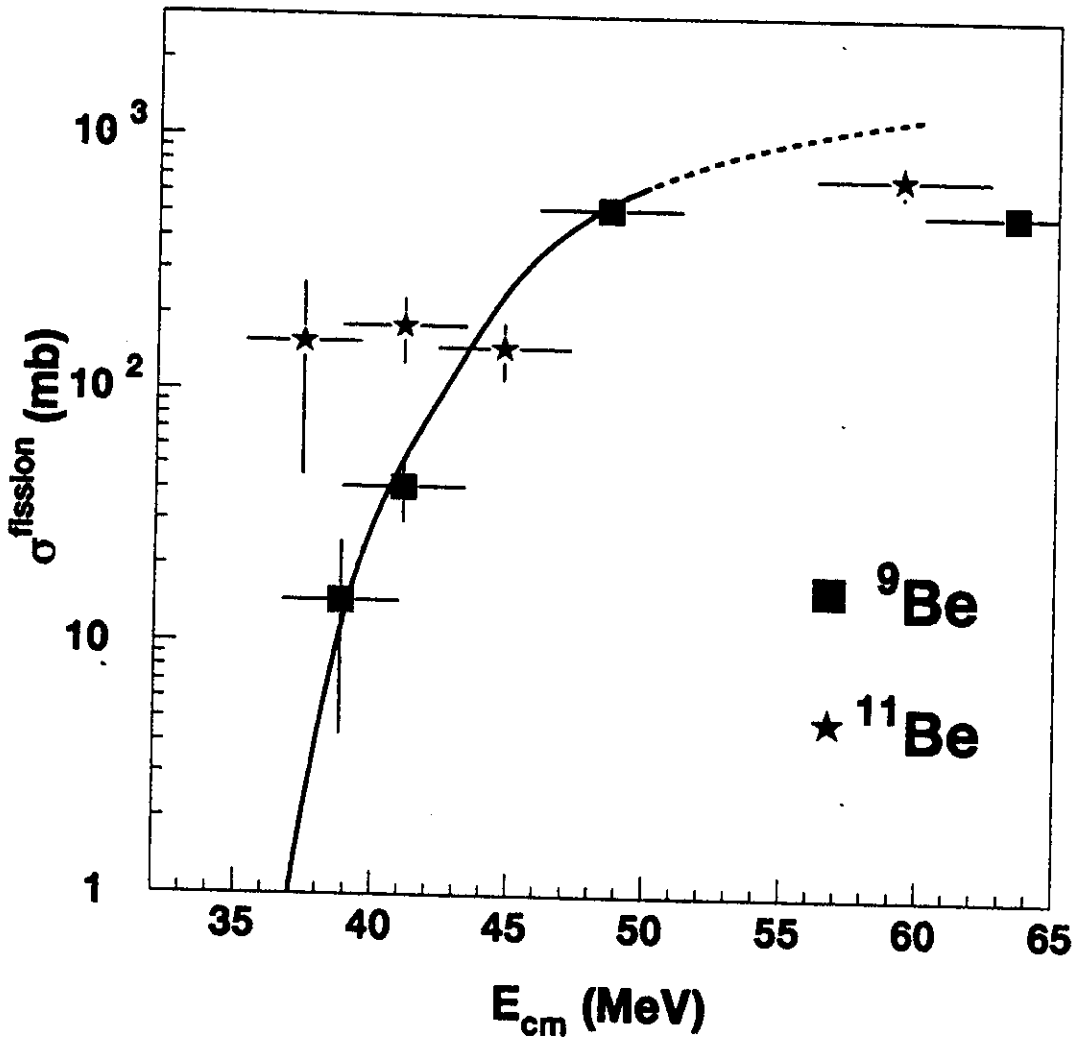
10^3
10^2
10
1
$\sigma^{fission}$ (mb)
35
40
45
50
55
60
65
E_{cm} (MeV)
^{9}Be
^{11}Be

Figure 8